PCCP

Accepted Manuscript

ROYAL SOCIETY OF CHEMISTRY

www.rsc.org/pccp

Cite this: DOI: 10.1039/c0xx00000x

www.rsc.org/pccp

ARTICLE TYPE

Topological analyses and small-world patterns of hydrogen bond networks in water + *t*-butanol, water + *n*-butanol and water + ammonia mixtures

Juliana Angeiras Batista da Silva,[a,b] Francisco George Brady Moreira,[c] Vivianni Marques Leite dos Santos[d] and Ricardo Luiz Longo*[b]

Received (in XXX, XXX) XthXXXXXXXXX 20XX, Accepted Xth XXXXXXXXX 20XX
DOI: 10.1039/b000000x

Cluster (or island) statistics and topological statistical mechanics based properties were employed in the analyses of hydrogen bond (H-bond) networks of *t*-butanol, *n*-butanol and ammonia aqueous solutions. These networks were generated from equilibrated Monte Carlo simulations at mixture compositions covering the entire range of miscibility and a fine grid of points around the topological transitions. We found that these H-bond networks changed from a percolation regime in water rich mixtures to a non-percolating behavior at non-aqueous component rich compositions. Topological analysis of local (clustering coefficients, average degrees) semi-global (path lengths) and global (spectral densities) properties indicated the presence of small-world patterns for the H-bond networks in mixtures at mole fraction compositions larger than *ca*. 0.6. These small-world patterns are characterized by highly clustered networks with small path lengths. Spectral densities show high order moment contributions that correlate with small-world patterns, thus corroborating the robustness of these statistical mechanics based topological analyses. The degree distributions of these networks were partially rationalized by the differences in the water-water and solute-solute H-bonds.

1. Introduction

The structures of fluids that interact by hydrogen bond (H-bond) are fundamental in many scientific, technological and natural processes. Water, being the liquid that sustains life and employed as green solvent is the most studied fluid containing H-bonds. Alcohols are also H-bonded fluids of interest because of their applications as solvents in chemical syntheses and separations. In particular, methanol and ammonia are used as prototypes for classes of more complex fluids. Most properties of H-bonded fluids are dictated by their H-bond networks. The mixture of two interacting liquids generates a network even more complex than their pure fluids. These types of mixtures are frequently used in many applications in chemistry and biology, especially water-alcohol mixtures, as solvents in various chemical and physical processes, whose properties can be adjusted simply by changing the mixture composition.[1,2,3] Thus, for example, it can control reaction rates, perform selective solvation, or change relative stabilities. Moreover in mixtures of solvents, especially when one of the components is water, chemical reactions can be strongly influenced by the solvent effects,[1,2,3] including the appearance of nonlinear behaviors.[4,5,6,7,8] In addition, mixtures of solvents can be used as a model for understanding hydrophobic/hydrophilic effects in more complex systems such as biomolecules in aqueous environments.

The intermolecular interactions (hydrogen bond, dipole-dipole, dispersion, close range repulsion, etc.) characteristics of liquids and solutions are key to understanding of their structures and dynamics, which depend mainly on the balance between these interactions and can lead to peculiar or anomalous behavior of several properties. However, collective and many-body effects also need to be taken into account for a proper description of liquids and mixtures. This can be performed by statistical mechanics approaches such as Monte Carlo and molecular dynamics for ensemble simulations. Whereas the properties of the complex H-bond networks should also be analyzed by statistical mechanics based methods.

Indeed, we have used these approaches to study the topology of H-bond networks in several systems. We have found small world patterns in supercritical water.[9] The H-bond networks of pure water and methanol also present a very rich behavior when the Coulomb contribution for the interaction potential is damped by a factor varying from 0 to 1.[10] Small-world patterns appear for the damping factor in the 0.60–0.75 range for both liquids. These patterns were characterized by the local (clustering coefficients, average degrees), semi-global (path lengths) and global (spectral densities) properties of the networks and by island statistics. Noteworthy that the small-world regime does not depend on the molecular structure of the liquid, which show that this topological behavior (small-world patterns) may be universal and it is intrinsically related to the networks themselves and not to their components. In contrast, quite distinct phase transitions of the macroscopic properties (mass density and vaporization enthalpy)

were obtained for these liquids and the critical values obtained from the thermodynamic properties coincide with those obtained from the topological analysis. This provides a relationship between some macroscopic properties and the topology of the H-bond networks. We have also investigated water-methanol mixtures.[11] Two distinct behaviors were uncovered from the island or cluster statistics, which were related to a change from a percolation regime for methanol mole fraction $x_m < 0.5$ to a non-percolating system for larger x_m, in good agreement with results available in the literature,[12,13,14,15] but obtained by different approaches. These results corroborated previous proposals based on experimental and/or molecular simulation data obtained by distinct techniques.[12,16] Also small-world patterns appear for x_m in the range 0.40–0.70, when the properties of the H-bond networks are analyzed. The spectral densities show several peaks, which also correlate well with rings, chains and branched chains topological features in water-methanol mixtures.

Small-world patterns were initially found in fully connected networks that were randomly reconnected (rewiring).[17] In a certain range of rewiring probabilities, it was uncovered that the number of connections was small for any given pair of nodes and the network presented large clustering coefficients compared to random graphs. Indeed, despite their often large sizes, distinct networks with clustering coefficients unusually large present a relatively short path between any two nodes, that is, small-world patterns.[18] In addition, it has been shown that small-world regimes interpolate between the highly clustered regular lattices (possibility, percolation regimes) and random graphs.[18] Finally, important properties of complex networks such as growth dynamics, resilience, evolvability, fitness, and robustness with respect to external fluctuations may be related to their topological properties, specially, to the small-world regimes.[18]

In the present work we employed topological analyses to characterize H-bond networks in liquids and mixtures (water-*t*-butanol, water-*n*-butanol, and water-ammonia) to evaluate the robustness and generality of those previous findings.[9-11] Thus, water-*t*-butanol and water-*n*-butanol mixtures are a natural extension of the water-alcohol systems for investigating, for instance, the effects of increasing bulkiness and of isomerism. Whereas studies of water-ammonia mixtures aim at ascertaining the effects of distinct hydrogen bond behaviors (strength and number) on the topological properties of these complex networks. More specifically, ammonia can form up to four hydrogen bonds (three H-donors/one H-acceptor), compared to two H-donors/two H-acceptors of water, and one H-donor/two H-acceptors of alcohols. In addition, these hydrogen bonds have quite different strengths. Thus, these mixtures should provide large variability for the H-bond networks and interesting testing grounds for topological analyses.

2. Methodology

Metropolis Monte Carlo simulations at normal conditions (1 atm, 298.15 K) were performed for water-*t*-butanol mixtures at 0.00, 0.10, 0.20, 0.25, 0.28, 0.30, 0.32, 0.36, 0.38, 0.42, 0.50, 0.60, 0.70, 0.80, 0.90, 1.00 *t*-butanol mole fraction ($x_{t\text{-but}}$) and for water-*n*-butanol mixtures at 0.00, 0.50, 0.55, 0.60, 0.65, 0.70, 0.75, 0.80, 0.85, 0.90, 1.00 *n*-butanol mole fraction ($x_{n\text{-but}}$). For water-ammonia mixtures, Metropolis Monte Carlo simulations were performed at 1 atm and 239.80 K, for 0.00, 0.10, 0.20, 0.25, 0.30, 0.40, 0.50, 0.60, 0.70, 0.80, 0.90, 1.00 ammonia mole fraction (x_a). Note that we are only interested in the region of miscibility with water, that is, the entire region of composition for water-*t*-butanol and water-ammonia mixtures, and for water-*n*-butanol mixtures outside the 0.02–0.49 range of *n*-butanol mole fraction. The results are compared with those obtained for water, methanol and water-methanol mixtures.[11]

The TIP5P model was used for water,[19] the six-site united-atom model (OPLS) for *t*-butanol and *n*-butanol[20,21,22] and all-atom model (OPLS-AA) for ammonia,[23] all of them at their respective molecular structure. The choice of these models is related to the sites (oxygen, nitrogen and hydrogen) that may form hydrogen bonds, namely, O-H in water and alcohols, and N-H in ammonia. For convenience and easiness of comparisons, the methyl groups were treated as united-atom models. The Lennard-Jones parameters between sites *i* and *j* at molecules of different types (e.g., water and ammonia) were obtained by the Lorentz-Berthelot combination rules: $\sigma_{ij} = (\sigma_{ii} + \sigma_{jj})/2$ and $\varepsilon_{ij} = (\varepsilon_{ii}\,\varepsilon_{jj})^{1/2}$, where σ_{ii} and ε_{ii} are the Lennard-Jones parameters of site *i*. For *n*-butanol a conformational analysis was performed using the RHF/6-311G* method and Monte Carlo search. The three most populated conformers for *n*-butanol were used in the mixtures with water. The structures of these conformers as well as the structure of all other molecules were kept rigid at their respective model geometries in all Monte Carlo simulations. This follows the Metropolis Monte Carlo simulation protocols used to derive the interaction potentials of the TIP5P and OPLS models. In addition, it avoids introducing unwanted variables in the analyses of the networks.

The simulations were performed with the DIADORIM program[24] using a cubic simulation box with 500 molecules. The simulation protocol employed periodic boundary conditions, a cutoff radius of 13 Å, an acceptance ratio of approximately 40%, and a trial volume variation was attempted every 2000 molecular move trials. For interactions beyond the cutoff radius, the reaction field method was used to describe the electrostatic interactions with a dielectric constant given by $(1 - x_s)\varepsilon_{water} + x_s\varepsilon_{pure}$, where x_s is the solute mole fraction and ε_{pure} denotes the dielectric constant for the pure liquid, namely, $\varepsilon_{water} = 80.0$, $\varepsilon_{t\text{-but}} = 10.9$, and $\varepsilon_{n\text{-but}} = 17.1$ at 298.15 K, $\varepsilon_{water} = 88.0$ and $\varepsilon_a = 22.0$ at 239.8 K. Equilibration was initially performed in the NVT ensemble with 10^7 configurations followed by 2×10^8 configurations in the NPT ensemble for each mole fraction. Averaging for the thermodynamic properties was then performed by generating 5×10^7 configurations.

The effects of considering the reaction field approach for long-range interactions and the number of MC steps between samples (statistically independent) have already been investigated.[11]

H-bonds between butanol molecules were defined by the same geometrical criteria used for methanol:[11] $R_{O\cdots H} \leq 2.60$ Å and $R_{O\cdots O} \leq 3.50$ Å, whereas between water and butanol molecules: $R_{Ow\cdots Obut} \leq 3.50$ Å and $R_{Ow\cdots Hbut}$ or $R_{Obut\cdots Hw} \leq 3.10$ Å,[25] where Ow, Obut, Hw and Hbut denote the oxygen and hydrogen atoms in water (w) and butanol (but) molecules, respectively. For H-bonds between ammonia molecules the geometric criteria were those used by Boese *et al.*[26]: $R_{N\cdots N} \leq 5.25$ Å and $R_{N\cdots Ha} \leq 2.70$ Å, while between water and ammonia molecules intermediate

criteria of water-water and ammonia-ammonia molecules were adopted: $R_{O\cdots N} \le 4.40$ Å, $R_{O\cdots Ha} \le 3.10$ Å and $R_{N\cdots Hw} \le 3.10$ Å, with Ha and Hw being the hydrogen atoms in ammonia (a) and water (w) molecules, respectively. In addition to these geometric conditions it is required that the interaction energy of the pair of molecules has to be negative (attractive) for the existence of an H-bond.

The information about which molecules are H-bonded is coded into a connectivity matrix that is used in the topological analysis. The topological properties[18,27] of the H-bond networks were determined by calculating the clustering coefficient C, the path length L, the degree distribution $P(k)$, and the graph spectra $\rho(\lambda)$ as were discussed previously and used for analyzing the water-methanol mixtures.[11] Because it is important to compare networks of very distinct origins (Internet, airline routes, electric power grids, social networks, collaborations, electronic circuits, phone call, citation, etc.)[18] to explore the universality of observed patterns, these topological properties are either dimensionless by definition or rescaled quantities. Usually this rescaling is performed with respect to the random graphs value or to the percolated network value. For instance, the path length measures the minimum number of connections between two given nodes and not the Euclidian or other metric distance. Whereas, spectral densities are conveniently rescaled with respect to analytical random graphs results to emphasize the differences between the network topological regimes.

The clustering coefficient of site (molecule) i, C_i, is defined as the ratio between the number of existing links (H-bonds), E_i, among the k_i neighbors of i and the total number that they would have if they formed a closed circle, i.e., $k_i(k_i-1)/2$.[18,27] The clustering coefficient, $\overline{C}$, of the entire network (simulation box) with N nodes (molecules) is then the average over all individual C_i's,

$$\overline{C} = \frac{1}{N}\sum_{i=1}^{N} C_i = \frac{1}{N}\sum_{i=1}^{N} \frac{2E_i}{k_i(k_i-1)} . \qquad (1)$$

The clustering coefficient of a simulated hydrogen-bonded liquid is obtained as the ensemble average, $C = \langle \overline{C} \rangle$, calculated over a given number (100 in the present case) of uncorrelated simulation boxes. For a random graph with N nodes and average degree $z = \langle \overline{k} \rangle$, the clustering coefficient is $C_{rand} = p = z/N$, because the links are distributed randomly with probability p.[18] According to the above relation for random networks the ratio C_{rand}/z scales as N^{-1}. However, real networks usually do not exhibit this dependence and some studies suggest that this ratio is independent of the number of nodes (N) in the network, as long as N is large enough. This property is characteristic of large networks whose clustering coefficients depend only on the coordination number (z) of the network and not on its size.[27]

The path lengths are determined as the ensemble average $L = \langle \overline{L} \rangle$ over uncorrelated networks, with the path length for a given network given by[27]

$$\overline{L} = \frac{1}{N}\sum_{i=1}^{N} l(i) . \qquad (2)$$

The path length or chemical distance of a given node i, $l(i)$, is determined from the shortest path lengths, $l_{min}(i,j)$, which are the minimum number of edges or links (H-bonds) connecting nodes (molecules) i and j within a cluster with N_i-nodes, namely,[27]

$$l(i) = \frac{1}{N_i}\sum_{j=1}^{N_i} l_{min}(i,j) . \qquad (3)$$

For a random graph, the path length scales logarithmically with the size of the network and, for $z > 1$,[18,27] where the average degrees (z) are always larger than 1 for all compositions analyzed,

$$L_{rand} \approx \frac{\ln N}{\ln z} . \qquad (4)$$

Therefore, a small-world pattern is characterized by $C >> C_{rand}$ and $L \le L_{rand}$.[18,27-30]

The topological properties and features explored so far are based mostly on local or semi-local type behavior. Whereas, spectral densities of the networks are based on global properties because the eigenvalues characteristic of the network are obtained by diagonalizing the $N \times N$ adjacency matrix $\boldsymbol{A}(G)$, with N being the number of nodes that involves the whole simulation box.[18,31] This matrix has elements $A_{ij} = A_{ji} = 1$ if nodes i and j are connected, and 0 otherwise and represents a graph G, whose spectrum is given by a set of N eigenvalues, λ_j, from which the spectral density can be obtained,

$$\overline{\rho}(\lambda) = \frac{1}{N}\sum_{j=1}^{N} \delta(\lambda - \lambda_j) . \qquad (5)$$

This spectral density approaches a continuous function as $N \to \infty$.[31] The spectral densities of the H-bond networks are averaged over an ensemble of uncorrelated simulation boxes to yield the spectral density, $\rho(\lambda) = \langle \overline{\rho}(\lambda) \rangle$. The number of paths returning to the same node in the graph is equal to the k-th moment of the spectral density, thus yielding a global topological feature of the network. More specifically, the topological features of graph can be directly related to the spectral density because its k-th moment can be written as the sum over the number of paths returning to the same node in the graph, where these paths may contain nodes that were already visited.[31]

If a network has N nodes linked randomly with probability p, the random graph corresponds to an infinite cluster as $N \to \infty$. In this case, the spectral density converges to a semicircular distribution given by,[18,31]

$$\rho(\lambda) = \begin{cases} \dfrac{\sqrt{4Np(1-p) - \lambda^2}}{2\pi Np(1-p)} & \text{if } |\lambda| < 2\sqrt{Np(1-p)}, \\ 0 & \text{otherwise} \end{cases} \qquad (6)$$

which is used to rescale the spectral density (ordinate) as

$$\rho(\lambda) \to \rho(\lambda) \times \left[Np(1-p)\right]^{1/2} , \qquad (7)$$

and eigenvalues (abscissa) of H-bond networks as,

$$\lambda \to \lambda / \left[Np(1-p)\right]^{1/2} . \qquad (8)$$

Networks that are not fully connected and/or have trees are

characterized by momenta of orders larger than zero, so that spectral densities are very useful to characterize and categorize networks from many different origins.

Clustering coefficients and path lengths are said to describe, respectively, local and global behaviors of the networks.[27] However, we consider path lengths as a semi-global property of a network because it involves the characteristic distance in a graph or cluster. In the small-world regime, the number of graphs is large and consequently their lengths should yield a semi-global description. That is another reason for calculating spectral densities because we claim that they do provide a global description of the network behavior, since the diagonalization of the adjacency matrix involves all nodes in the network.

The topological properties as well as the histograms in the island statistics were obtained as configurational (ensemble) averages over 100 samples collected every 10^4 configurations (20 MC steps). This was the same sampling used in the investigation of H-bond bond topological properties of water-methanol mixtures.[11] It was shown that these structures were statistically uncorrelated because when the number of configurations between the collected samples was systematically increased, the averaged topological properties remained unaffected.[11] In addition, averages over larger samples, *e.g.* 500, yielded the same results, so for practical reason, mainly in the calculation of the spectral density, averages over 100 samples were used.

The computer program[11] coded for performing the topological analysis was used and performs the following tasks: reads the coordinates of the molecules in the simulations boxes, determines which molecules (including their type) are connected by hydrogen bonds, builds the connectivity matrix (or adjacency matrix) and then calculates the topological properties and performs the island statistics.

3. Results and discussion

The calculated thermodynamic (density, enthalpy of vaporization, heat capacity, etc.) and structural properties (radial distribution functions - RDFs), for the pure liquids and the mixtures are in excellent agreement with available experimental and simulated values in the literature.[9,13,16,19,20,23,25,32-46] These results ensure that the simulation protocol used is appropriate as extensively checked previously in the simulations of water-methanol mixtures.[11] Moreover the RDFs are consistent with the distance criteria used for determining the hydrogen bond between two molecules. Regarding the dependency of properties such as density and vaporization enthalpy with the solute mole fraction, x_s, we have observed a monotonic decrease for all mixtures analyzed. In water-*t*-butanol mixtures, both properties present an inflexion (maximum value) at concentration $x_{t\text{-but}} \approx 0.05$. This behavior is characteristic of the presence of clathrates as observed in earlier simulations and experimental measurements.[45,46] In the pure liquids, the average pair interaction energies between molecules are: for water molecules (–10.16 kcal/mol at 298.15 K and –11.43 kcal/mol at 239.80 K), *t*-butanol molecules (–11.52 kcal/mol), *n*-butanol molecules (–12.35 kcal/mol) and ammonia molecules (–4.12 kcal/mol). The corresponding values for *t*- and *n*-butanol molecules are more negative (attractive) than that for ammonia molecules, which is consistent with the strength and number of hydrogen bonds that these molecules are capable of forming. As has been pointed out in our previous work for water-methanol mixtures,[11] it should be expected that the structure of the first solvation shell remains unchanged at room temperature for *t*- and *n*-butanol (and at 239.80 K for water-ammonia) mixtures.

The structural features of the pure liquids and the mixtures were also in excellent agreement with available experimental data[16,37,47-50] and computer simulations[13,26,32,34,37,39,42] even with different intermolecular potentials and using a limited number of conformers in the simulations of water-*n*-butanol mixtures and *n*-butanol liquid.

3.1 Numbers and patterns of hydrogen-bonds: island statistics

The average degrees, z, for pure liquids ($x_s = 1$ in Figure 1) are in good agreement with available results, namely, $z_{t\text{-but}} \approx 2$ and $z_{n\text{-but}} \approx 2$ inferred from the work of Ferrari *et al.*,[37]. Gao *et al.*[32] and Ferrario *et al.*[39] estimated slightly different values for the average connectivity of ammonia, 2 and 3 bonds per molecule ($z_a \approx 2$-3[42,32,39]), from the radial distribution function.

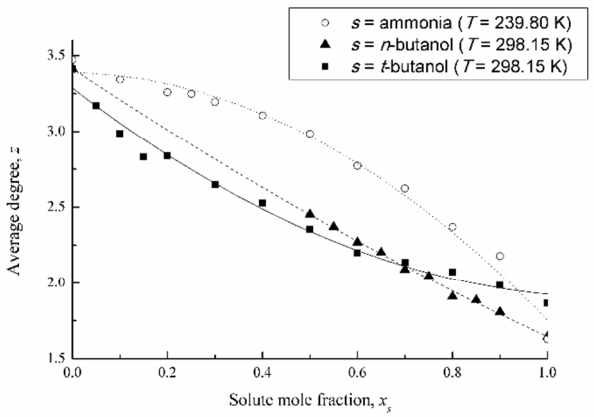

Fig. 1 The dependence of the average degree on the solute mole fraction x_s. The curves represent quadratic fit to the data.

Molecular dynamics simulation using different methods,[26,51] found that the ammonia molecules generally accept two molecules that interact by binding to two hydrogen atoms per molecule, which agrees with our results. Fig. 1 shows the average degree as a function of mole fraction of solute. For all aqueous mixtures studied, this property is a decreasing function of x_s. The results in Fig. 1, fitted to a quadratic function, show that water-*t*-butanol and water-ammonia mixtures have larger contribution of the quadratic term, namely, $z_{t\text{-but}} = 3.28 - 2.42x_{t\text{-but}} + 1.06x_{t\text{-but}}^2$ (R^2 = 0.985) and $z_a = 3.38 - 0.05x_a - 1.58x_a^2$ (R^2 = 0.986), compared to water-*n*-butanol $z_{n\text{-but}} = 3.41 - 2.09x_{n\text{-but}} + 0.32x_{n\text{-but}}^2$ (R^2 = 0.999) and water-methanol mixtures $z_m = 3.38 - 2.26x_m + 0.55x_m^2$ (R^2 = 0.997) obtained previously.[11] The increase of the relative contribution of the quadratic term may be related to a decrease of the interaction strengths of the H-bonds in the water-ammonia mixtures and to an increase of the steric effects in the water-alcohol mixtures. However, the number H-bond networks analyzed is too small to attach any definitive physical-chemical interpretation and/or rationalization to the dependence of the cluster statistics on the mole fraction.

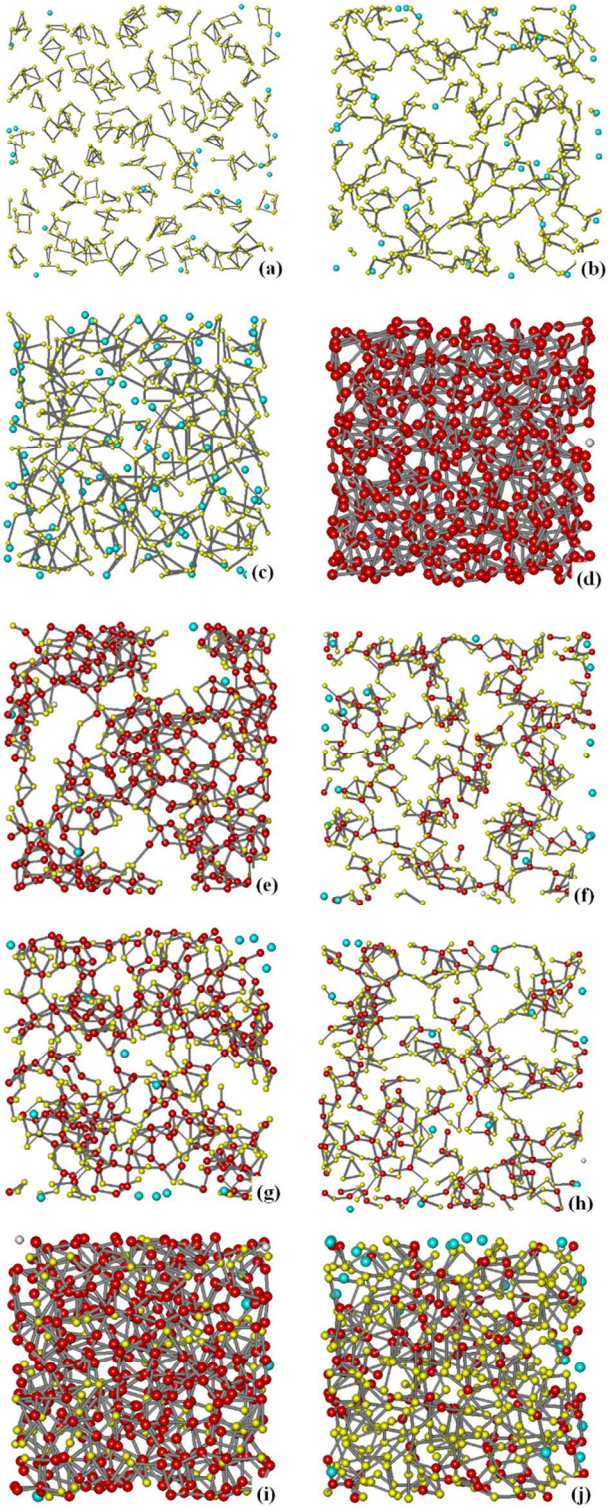

Fig. 2 Sphere-and-stick representation of the H-bond networks in (a) pure *t*-butanol; (b) pure *n*-butanol; (c) pure ammonia; (d) pure water; (e) $x_{t\text{-but}}$ = 0.30; (f) $x_{t\text{-but}}$ = 0.70; (g) $x_{n\text{-but}}$ = 0.50; (h) $x_{n\text{-but}}$ = 0.70; (i) x_a = 0.30 and (j) x_a = 0.70. All results involving alcohols were obtained at 298.15 K, pure water and ammonia at 239.80 K. Each node (sphere) represents one molecule and the edges (sticks) the hydrogen bonds. The red and yellow balls represent H-bonded water and solute, respectively, whereas isolated (non-connected) nodes (molecules) are shown as white (water) and light blue (solute) spheres.

The networks formed by hydrogen bonds in pure liquids and some values of x_s for mixtures can be inspected visually by sphere representations[13] or as we prefer the sphere-and-sticks representation in Fig. 2. Each molecule (or node) is represented by a site of interaction of the network, which is represented in the graphs of the figures only by the center of mass of each molecule. The existing H-bond interaction between two molecules is represented by a line (or stick). We have chosen to analyze snapshots of the mixtures at mole fractions that were the most representative to their topological behaviors. Additional snapshots at solute mole fraction of 0.5 are presented in the Supplementary Information (Figure S2). Although these 2D representations are rather limited, some conclusions can be inferred from their observations. For example, different aggregation modes are observed for the two isomers of butanol. In pure *t*-butanol (Fig. 2a), the H-bond network consists mainly of rings of different sizes, with the *t*-butyl groups (not shown) pointing away from the rings due to steric hindrance. While in pure *n*-butanol (Fig. 2b), long chains of H-bond interactions are formed. Ammonia (Fig. 2c) at 239.80 K has a large number of isolated molecules and molecules with one or two connections, while the H-bond network in water at the same temperature (Fig. 2d) is highly connected and practically all molecules belong to a giant cluster. Previous results[11] showed that the network formed by water molecules at room temperature is in the percolation regime. Whereas previous analyses[11] of liquid methanol showed aggregates of different sizes, a few isolated molecules and large void spaces that suggest the formation of hydrophobic pockets with the methyl groups filling these.

For aqueous mixtures it is observed the presence of highly connected clusters and empty regions that increase with the water contents. Comparison of the results for water-*t*-butanol mixtures with those for water-methanol mixtures[11] (Fig. 2e and 2f) shows that there is a large difference regarding the homogeneity within these networks. It is worth mentioning that both methanol and *t*-butanol have the same number of H-bond interaction sites, but there is a difference on their clustering coefficients (section 3.2) obtained for these pure liquids. The water-*n*-butanol mixtures (Fig. 2g and 2h) visually resemble the water-*t*-butanol. For water-ammonia mixtures the figures 2i and 2j show that the networks are quite connected, making it even more connected as increasing the molar fraction of water in the mixture.

For these mixtures is more difficult to analyze the percolation behavior only by visual analyses than for the water-methanol mixtures. Thus, the same statistical tools were applied for these systems, that is, island statistics[28] by analyzing the average sizes of the largest islands or clusters (N_{li}) as a function of composition, as well as the bin distribution of islands, namely, the number of islands, n_s, with s components in the interval $[2^{bin-1}, 2^{bin} - 1]$. The average number of components in the largest island (cluster), N_{li}, for all compositions investigated is shown in Fig. 3.

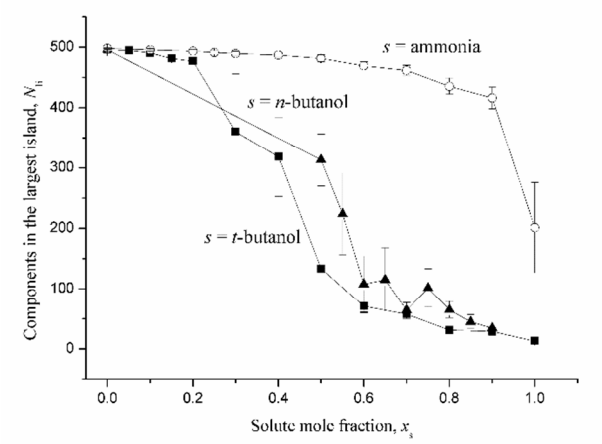

Fig. 3 Average number of components in the largest island (cluster), N_{li}, as a function of the solute mole fraction x_s, where the bars indicate the standard deviations. All results involving alcohols were obtained at 298.15 K and ammonia at 239.80 K

For all mixtures, the number of components in the largest island decreases with the solute mole fraction, x_s. The water-*t*-butanol mixtures show a smoother percolation transition, which causes difficulties in determining the critical value. Because *n*-butanol is miscible in water only when its mole fraction is larger than 0.45, the non-percolating regime cannot be determined. The water-ammonia mixtures showed that even small quantities of water in the mixtures cause the network to percolate, in contrast to pure liquid ammonia that has a large number of small clusters and monomers. These results were quite different from those obtained for water-methanol mixtures, where a drastic change in the average number of components in the largest cluster was observed at methanol mole fraction $x_m = 0.50$, leading to a non-percolating regime at higher methanol concentrations.

Figure 4 presents the quantitative results for the bin size analysis by plotting the number n_s of islands (clusters) with s molecules in the range $[2^{bin-1}, 2^{bin} - 1]$ for several mixture compositions of the systems studied. For pure *t*-butanol (Fig. 4a) there is a predominance of aggregates containing 2-7 molecules, while for the pure *n*-butanol (Fig. 4b) there is approximately the same number of monomers, however with a variety of larger aggregates with different sizes. Again, it is observed a clear distinction in the aggregation of the molecules of the isomers butanol. Liquid ammonia (Fig. 4c) contains about 15% of monomers, in agreement with the value obtained by Ibrahim and Jorgensen[42] and 5% of dimers and trimers, the value obtained also by Ricci *et al.*[52] In water at normal conditions (Fig. 4a and 4b) there is a giant cluster with about 99% of the molecules and at lower temperatures (Fig. 4c) approximately all molecules belong to the large island. The mean values of the sizes of the largest islands (Table 1) are in agreement with these observations.

The island statistics of the mixtures exhibits behaviors intermediate between those of the pure liquid constituents. For water-*t*-butanol mixtures (Fig. 4a) as $x_{t\text{-but}}$ increases, the percolating aggregate in pure water disintegrates in the following way: *i*) for $x_{t\text{-but}} < 0.3$ there are a few isolated molecules and small aggregates, with most of molecules belonging to the giant aggregate; *ii*) when $x_{t\text{-but}} \geq 0.3$, it is also observed the formation of a giant aggregate containing more than 50% of the molecules, however, the number of smaller aggregates becomes greater; and *iii*) for $x_{t\text{-but}} \geq 0.6$, there are aggregates of various sizes, containing from 1 to 127 molecules.

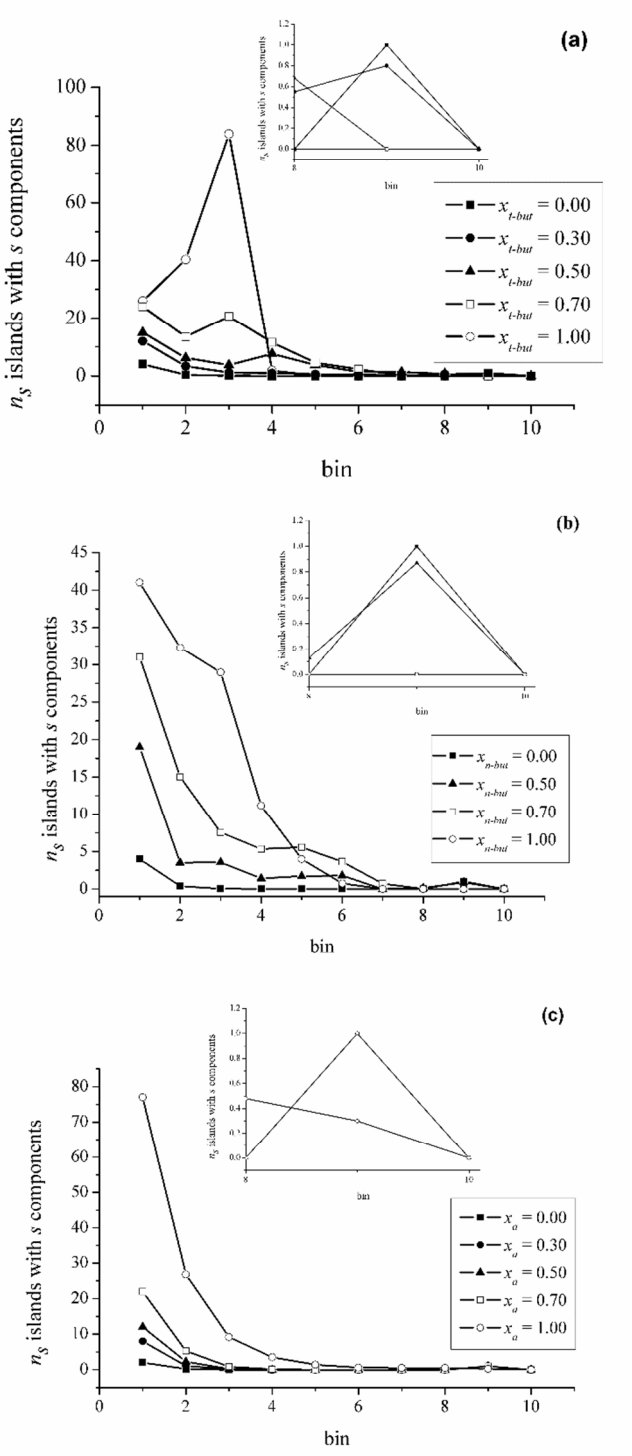

Fig. 4 Island statistics counts the number of clusters (islands) of sizes s in the interval $[2^{bin-1}, 2^{bin} - 1]$ for each bin. The dependence with the mixture composition is shown at several solute mole fraction x_s, for (a) s = *t*-butanol at 298.15 K, (b) s = *n*-butanol at 298.15 K, and (c) s = ammonia at 239.8 K. The insets are magnifications of the region around bin = 9.

The water-*n*-butanol mixtures present similar behavior of the water-*t*-butanol ones, with a peculiar distinction related to the formation of clusters containing 4 to 7 molecules of *t*-butanol at high values of the *t*-butanol mole fraction (Fig. 4b), which may be attributed to the formation of rings, as can be seen in Fig. 3a. At all compositions of water-ammonia mixtures (Fig. 4c) there is a large island containing 50-100% of the molecules, whose size varies with the composition. Pure liquid ammonia, as discussed early, has a variety of islands of different sizes. All these observations are directly related to the number of components found in the largest island (N_{li}) that decreases with increasing x_s (Fig. 3).

3.2 Clustering coefficients and path lengths: small-world patterns

The intermediate behavior of networks between random and regular networks may lead to small-world patterns in complex networks. Properties such as clustering coefficients and path lengths have been used to analyze these behaviors. For example, in random networks the clustering coefficients are smaller and the path lengths are longer than those in regular networks, which have large clustering coefficient and path lengths that grow linearly with the number of nodes (N). Small-world patterns are characterized by an intermediate behavior having large clustering coefficients (like regular networks) and smaller path lengths than random networks.

Table 1 Path length (L), clustering coefficient (C), average degree (z) and the number of components in the largest island (N_{li}) for the pure liquid networks and for the corresponding random networks (rand).

	L	L_{rand}	C	C_{rand}	z	N_{li}
Water at 298.15 K[a)]	17.67	5.06	0.0418	0.0068	3.413	495.84
Methanol at 298.15 K[a)]	5.15	12.30	0.0071	0.0033	1.657	50.37
t-Butanol at 298.15 K	3.12	9.95	0.2570	0.0037	1.867	12.76
n-Butanol at 298.15 K	4.61	12.52	0.0473	0.0033	1.642	33.34
Ammonia at 239.80 K	4.09	12.74	0.0221	0.0033	1.628	201.02
Water at 239.80 K	17.88	4.99	0.0223	0.0070	3.471	497.95

[a)] ref. [11]

Table 1 shows the results of topological properties such as chemical distance or path length (L), clustering coefficient (C), average connectivity (z) and the number of components of the largest island (N_{li}) in networks of hydrogen bonds formed by pure liquids. Also reported are the values of the chemical distance (L_{rand}) and the clustering coefficient (C_{rand}) of the corresponding random networks, namely, random networks with the same number of nodes and average degree. These properties were obtained with errors of less than 2%, except for the calculation of the clustering coefficient due to the great diversity of types of the clusters whose deviations were around 10%.

The different modes of aggregation for the isomers of butanol that were observed qualitatively by viewing equilibrated box simulations can be quantified by the clustering coefficient that is greater for *t*-butanol (reflecting formation of rings) than for *n*-butanol (large number of chains). For the same temperature, pure water has clustering coefficients very similar to those in pure *n*-butanol and ammonia; however, the water average degrees are more than twice of *n*-butanol and ammonia. This behavior can be expected since the link (i.e., the interaction by hydrogen bond) between neighboring molecules (that defines the clustering coefficient) only occur at appropriate distance and orientation (which depend on the criteria for determining the hydrogen bond) and thus steric effects, the number of sites for the formation of hydrogen bond per molecule and bond strength are important factors.

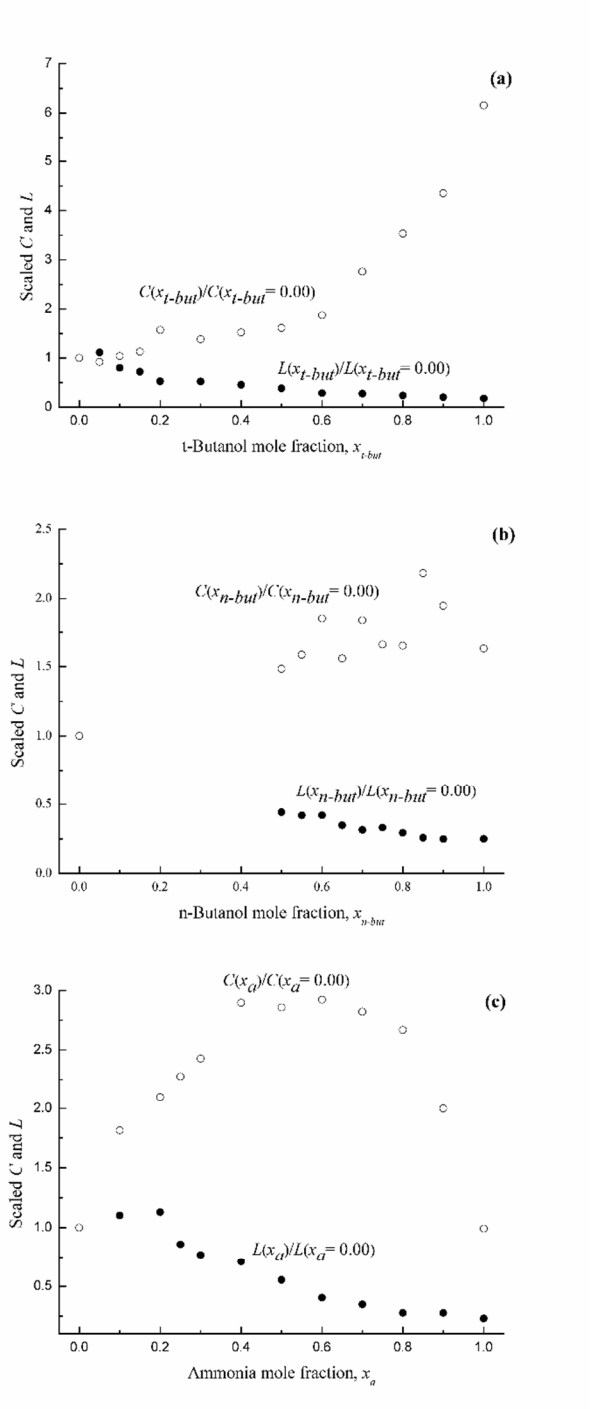

Fig. 5 Clustering coefficients (C) and path lengths (L) scaled by their values at $x_s = 0.0$ as a function of the solute mole fraction, x_s: (a) s = *t*-butanol at 298.15 K; (b) s = *n*-butanol at 298.15 K; (c) s = ammonia at 239.80 K.

Also from Table 1 it is observed that in the networks formed by the isomers of butanol and ammonia, the values of the clustering coefficients (C) is much larger than the corresponding ones in random networks (C_{rand}) with the same connecting probability (p), that is, $C >> C_{rand}$. The path lengths have an opposite behavior, namely, they are smaller for real networks (L) than the associated random ones (L_{rand}), i.e. $L < L_{rand}$. These two conditions characterize the small-world behavior of these networks. Notice that pure water at either temperature as well as liquid methanol did not present this small-world behavior of their H-bond networks. Indeed, only in a certain concentration range of methanol-water mixtures a small-world regime was observed.

The transition between regular and random networks, namely the small-world behavior may be characterized by the clustering coefficients, $C(x_s)$, and path lengths, $L(x_s)$, as functions of the mixture composition (x_s) and scaled by their respective values at $x_s = 0.0$, that is, $C(x_s)/C(x_s = 0.0)$ and $L(x_s)/L(x_s = 0.0)$, which are depicted in Fig. 5.

The choice of normalization by the respective values at $x_s = 0.0$, which correspond to the values obtained for pure water, can be justified as the only common component in the mixtures to allow for comparisons, and also not to display small-world patterns. Comparisons with the Watts-Strogatz model[17] must be performed carefully because the standardization is done in the model for the probabilities for reconnection (p) equal to zero and therefore in this condition, the system corresponds to a regular network. Noteworthy that all values of p studied in the Watts-Strogatz model, the average degree is constant. Thus, to validate our choice for the normalization factor, the clustering coefficients and the path lengths are compared with the values of the corresponding random networks (rand). For non-normalized values see Fig. S3 in the Supplementary Information.

Outside the region of small-world patterns the networks of H-bonds have $L > L_{rand}$ and $C >> C_{rand}$, which suggests that the path lengths of the network increase with its clustering coefficients, characteristic of a giant cluster that percolates the system.[18] In the region of small-world regime, the opposite behavior is observed, where the networks possess much smaller path lengths $L < L_{rand}$, while the clustering coefficients are still large $C >> C_{rand}$.[17] These regions are detected in either the scaled graphs in Fig. 5 or in comparisons between the values in real networks and the corresponding values for the random networks (Fig. S3 in the Supplementary Information). These observations validate our choice of the normalization factor.

Small-world patterns were found in the H-bond networks of all aqueous mixtures analyzed at specific intervals of compositions.

For the water-*t*-butanol mixtures, there is a steeply increase of the clustering coefficients from $x_{t\text{-but}} \geq 0.6$, whereas the path lengths decrease steadily up to $x_{t\text{-but}} \approx 0.6$ and remain approximately constant beyond this composition. Our results corroborate previous molecular dynamics simulation results obtained by Ferrari *et al.*[37] that observed the formation of *t*-butanol dimmers in aqueous *t*-butanol solutions at high water content, namely, the region at which small clustering coefficients are obtained. It was also observed that at $x_{t\text{-but}} = 0.6$, the alcohol molecules form rings instead of chains as the main mode of aggregation of the water-*t*-butanol systems, which is reflected by the observed increase in clustering coefficient values for $x_{t\text{-but}} \geq 0.6$. The scaled graph obtained by normalizing with the respective values of these properties at $x_{t\text{-but}} = 0.0$ (Fig. 6) and comparisons of these properties with the corresponding values for random networks (Fig. 7) show that for this system, only solutions rich in *t*-butanol, as well as pure liquid *t*-butanol, have small-world patterns. Following the same analysis, water-*n*-butanol mixtures also present small-world behaviors for solutions rich in *n*-butanol and in pure *n*-butanol.

Water-ammonia mixtures also show small-world patterns, although the clustering coefficient presents values up to three times higher in the mixtures than in pure water or pure ammonia (Fig. 5c). Note that these properties were obtained at 239.80 K and therefore the value of the clustering coefficient for the pure water at this condition, i.e. at $x_a = 0.0$, is different from the value at $x_{t\text{-but}} = 0.0$ or $x_{n\text{-but}} = 0.0$ at room temperature. Probably due to intrinsic characteristics of the H-bonds in these systems, for example, the existence of three different types of interactions with distinct relative strengths (water-water, water-solute and solute-solute), the topological properties did not exhibit a regular behavior, as observed previous studies.[11]

The scaled or unscaled clustering coefficients in the pure liquid ($x_s = 1$ in Figures 5 and S3) have the following trend: $C_{t\text{-butanol}} >> C_{n\text{-butanol}} > C_a$. This trend may be rationalized by inspecting Figures 3a, 3b and 3c that show the H-bond networks of pure *t*-butanol, *n*-butanol, and ammonia, respectively. It is clear that liquid *t*-butanol presents many rings of several sizes, whereas rings are scarce in pure *n*-butanol and practically inexistent in ammonia. Because the clustering coefficients are related to the connections between the neighbors of a given site, eq. (1), the presence of rings should lead to larger clustering coefficients compared to networks where the presence of rings is rare.

Combining the results from the island statistics with local topological properties (path length and clustering coefficient) it is possible to infer that transition from the percolation to the small-world regimes occur at mole fractions larger than *ca*. 0.6 for the water-alcohol mixtures. Interestingly, in water-ammonia mixtures highly connected H-bond networks still present for ammonia mole fraction up to 0.7; however, small-world patterns start to emerge at $x_a \approx 0.3$. Thus, a clear transition from the percolation to the small-world regimes in water-ammonia mixtures is difficult to pinpoint without a more detailed application of percolation theory, which is outside the scope of the present analyses.

3.3 Degree distribution: broad-scale networks

The number of neighbors of a given molecule, and thus its number of H-bond connections, changes continuously due to the thermal motions in the liquids. So, a distribution of the number of H-bonds in an instantaneous configuration of the mixture is to be expected. After normalization, this distribution leads to the degree distribution, $P(k)$, which yields the frequency of nodes (molecules) that have k connections (H-bonds). As in the case of other H-bond network properties, $P(k)$ is also a parametric function of the mixture composition, that is, $P(k; x_s)$.

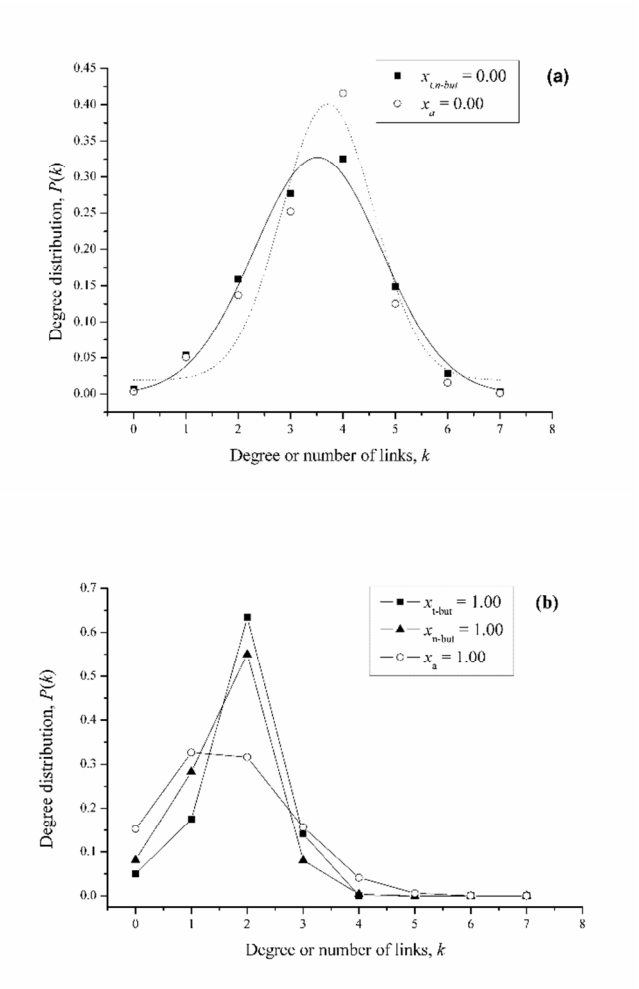

Fig. 6 Degree distribution, $P(k)$, for pure liquids: (a) water at 298.15 K ($x_{t,n\text{-but}} = 0.00$) and at 239.80 K ($x_a = 0.00$); (b) *t*-butanol, *n*-butanol and ammonia. In (a) the solid and dotted curves are Gaussian functions fitted to each data set.

Fig.6 presents the degree distribution for selected values of x_s. The networks have degree distributions that deviate significantly from a Poisson distribution and as a result, do not show the random networks behavior. Pure water at 298.15 K and 239.80 K has fully connected networks displaying an approximated single-scale (Gaussian) distribution, which are similar random graphs (Fig. 6a). At room temperature, the degree distribution, $P(k; x_s = 0)$, of liquid water is fitted to a Gaussian distribution with a slightly better accuracy than water at 239.80 K. These fitted functions have an average connectivity of 3.52 and 3.71, and widths equal to 2.44 and 1.77 at 298.15 K and 239.80 K, respectively. In contrast, pure liquid alcohols show a sharp peak at $k \approx 2$, in agreement with previous simulations carried out for the methanol[23,41,39] and a fast decay for $k > 2$ (Figs. 6b, 7a and 7b). The degree distributions decay as a power law followed by a cutoff, that is, $P(k) \approx k^{-\gamma} f(k/k_{cutoff})$, where k_{cutoff} is the cutoff for the number of connections or hydrogen bonds. The estimated values of the exponents γ are 9.46 for *t*-butanol and 8.66 for *n*-butanol, both with $k_{cutoff} \approx 4$, with $R^2 \approx 0.92$-0.97. This behavior of the degree distributions is expected for a class of small-worlds known as broad-scale networks, which are characterized by a limiting constraint for the addition of new connections.[29] Ammonia has a degree distribution with a smooth decay (Figs. 6b and 7c) with about 15% of the molecules with one connection, 20% with four or more connections and 65% with two-three H-bonds, in good agreement with the results obtained by previous simulations.[32]

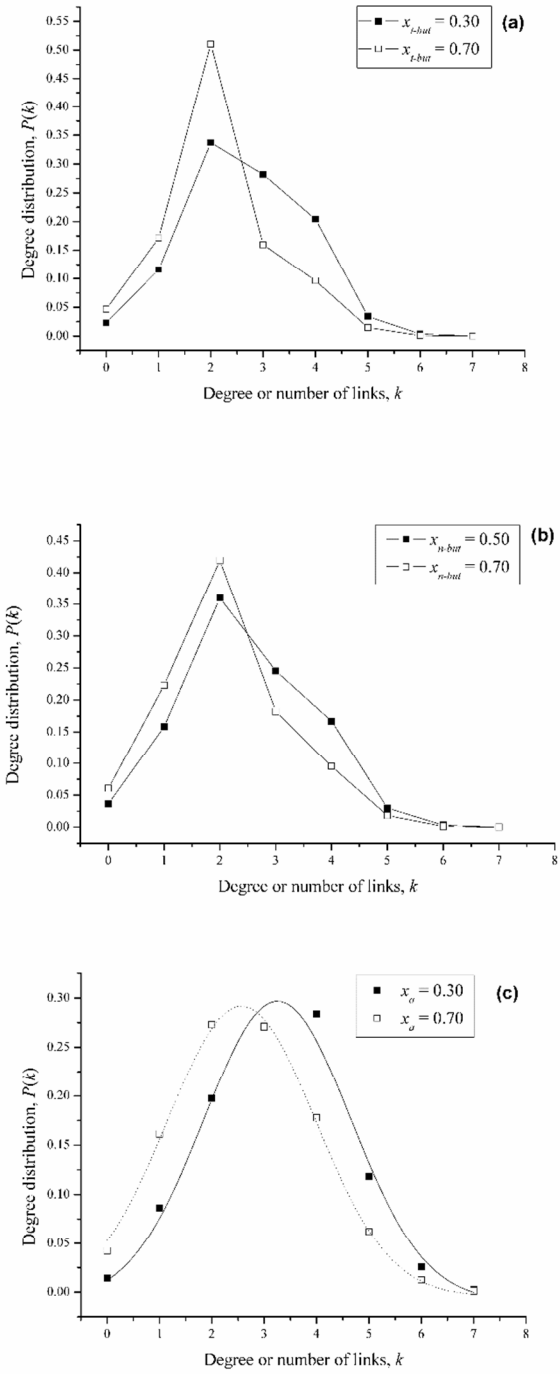

Fig. 7 Degree distributions, $P(k)$, for selected compositions of water-solute (s) mixtures (a) s = *t*-butanol at 298.15 K, (b) s = *n*-butanol at 298.15 K, and (c) s = ammonia at 239.80 K. In (c) the solid and dotted curves are Gaussian functions fitted to each data set.

These distinct behaviors of the pure liquid networks suggest that the H-bond networks in the mixtures should present composition dependent degree distributions, $P(k)$, as shown in Fig.7. For the water-*t*-butanol mixtures, it was observed that regions rich in water present a very wide distribution of connectivities while for $x_{t\text{-but}} \geq 0.6$ the distributions become more narrow and symmetric. This behavior can be attributed to the presence of a large number of rings and because the average connectivity of the molecules in a ring is equal to 2, the maxima of the distributions also occur at $k \approx 2$. Water-*n*-butanol mixtures present similar behavior, but in these cases, there are a large number of chains, including branched chains ($k > 2$) that lead to a broadening of the distribution for $k > 2$ as the *n*-butanol mole fraction increases.

Similarly to the water-methanol mixtures,[11] there are compositions of water-*t*-butanol and water-*n*-butanol mixtures where small-world patterns are detected with degree distributions that are characteristics of broad-scale networks with a sharp cutoff. This is consistent with the conjecture that the broad-scale distribution is due to the high cost of connections within a network,[29] as can be seen in the Figs. 7a and 7b at $x_s = 0.7$. The formation of networks with this type of degree distribution in a *t*-butanol rich environment can be attributed to the large steric hindrance of the *t*-butyl group that leads to smaller number of interaction sites for H-bonds and weaker strengths of these interactions.

These behaviors of water-alcohol mixtures, including methanol, can be rationalized by the smaller number and the weaker interaction of the H-bonds formed by alcohol molecules compared to those of water. Therefore, replacing water by alcohol molecules in H-bond networks causes an abrupt decrease of connectivity and a sharp cutoff of the degree distribution. In addition, steric effects of the alkyl chains in the alcohol molecules hinder the H-bond connections and contribute to the sharper cutoff of the *t*-butanol degree distribution compared to *n*-butanol mixtures (Figs. 7a and 7b).

For water-ammonia mixtures at $x_a = 0.7$ and 0.3 (Fig. 7c), the data sets of the degree distributions were fitted to Gaussian functions with average connectivities of 2.57 and 3.26, respectively. This behavior of the degree distributions is consistent with small-world networks characterized as single-type scale.

3.4 Spectral densities

The rescaled spectral densities of H-bond networks for all mixtures were obtained and are depicted in Figs. 8 and 9 for selected compositions. At both temperatures, pure water presents spectral densities dominated by the first moment (Fig. 8a), as expected from the observed percolation behavior, that is, the formation of a giant cluster that contains most molecules. Similar behavior is observed for low values of the solute mole fraction in which the spectral densities are dominated by the first moment (Figs. 9a, 9c and 9e), but the semicircular shape is suppressed when the solute mole fraction increases. On the other hand, for larger values of x_s, including the pure liquids, the spectral densities have significant contributions from the second and third moments (Figs. 8b, 9b, 9d and 9f), which is consistent with the small-world behavior of these H-bond networks and the presence of a large number of isolated clusters. Notice that the higher moments appear only because we employed a cutoff when the spectral densities were plotted in order to provide more details. In fact, the principal peaks reach 0.7 in the scaled spectral density axis, so that the observed moments for low solute mole fractions are negligible. However, for larger mole fractions these momenta are significant.

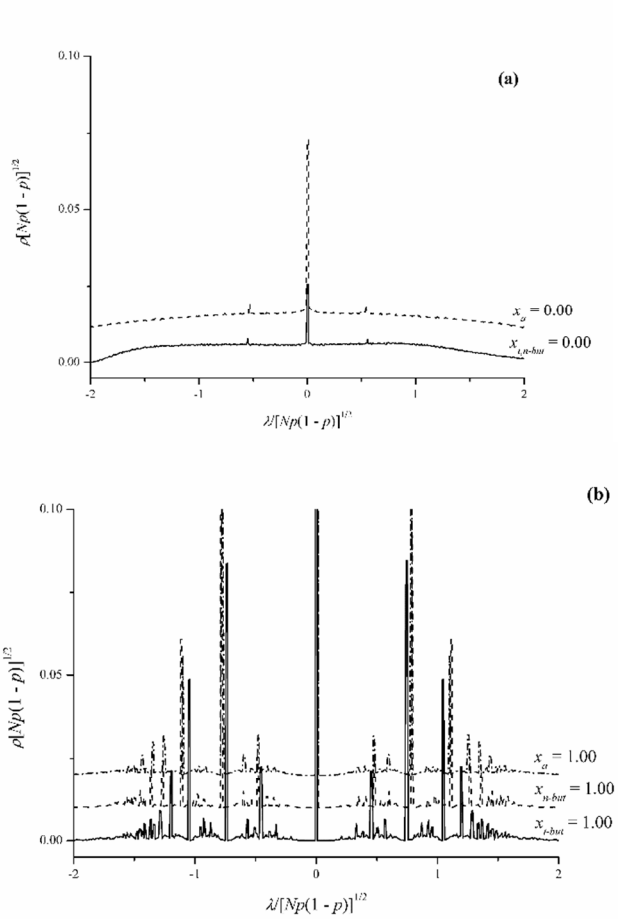

Fig. 8 Rescaled average spectral densities of H-bond networks in pure liquids: (a) water at 298.15 K ($x_{t,n\text{-but}} = 0.00$) and 239.80 K ($x_a = 0.00$); (b) *t*-butanol at 298.15 K, *n*-butanol at 298.15 K and ammonia at 239.80 K. The cutoff value of 0.1 was used in the scaled spectral density in order to show more details. The spectral density of water at 239.80 K in (a) was shifted by 0.01 for better visualization. The spectral densities of *n*-butanol and ammonia in (b) were shifted by 0.01 and 0.02, respectively, for better visualization.

In summary, cluster statistics, local, semi-global and global topological properties clearly show the small-world patterns in the H-bond networks of all aqueous mixtures studied in a wide range of solute concentration. These observations suggest that small-world topologies of these networks are common and, probably, general, which may be due to the special features of small-world networks, namely, fast transport of information and communication.[18] These features may account for the robustness and resilience of these H-bond networks with respect to perturbation and thus correlated to the miscibility and solution stability.

Cite this: DOI: 10.1039/c0xx00000x

www.rsc.org/pccp

ARTICLE TYPE

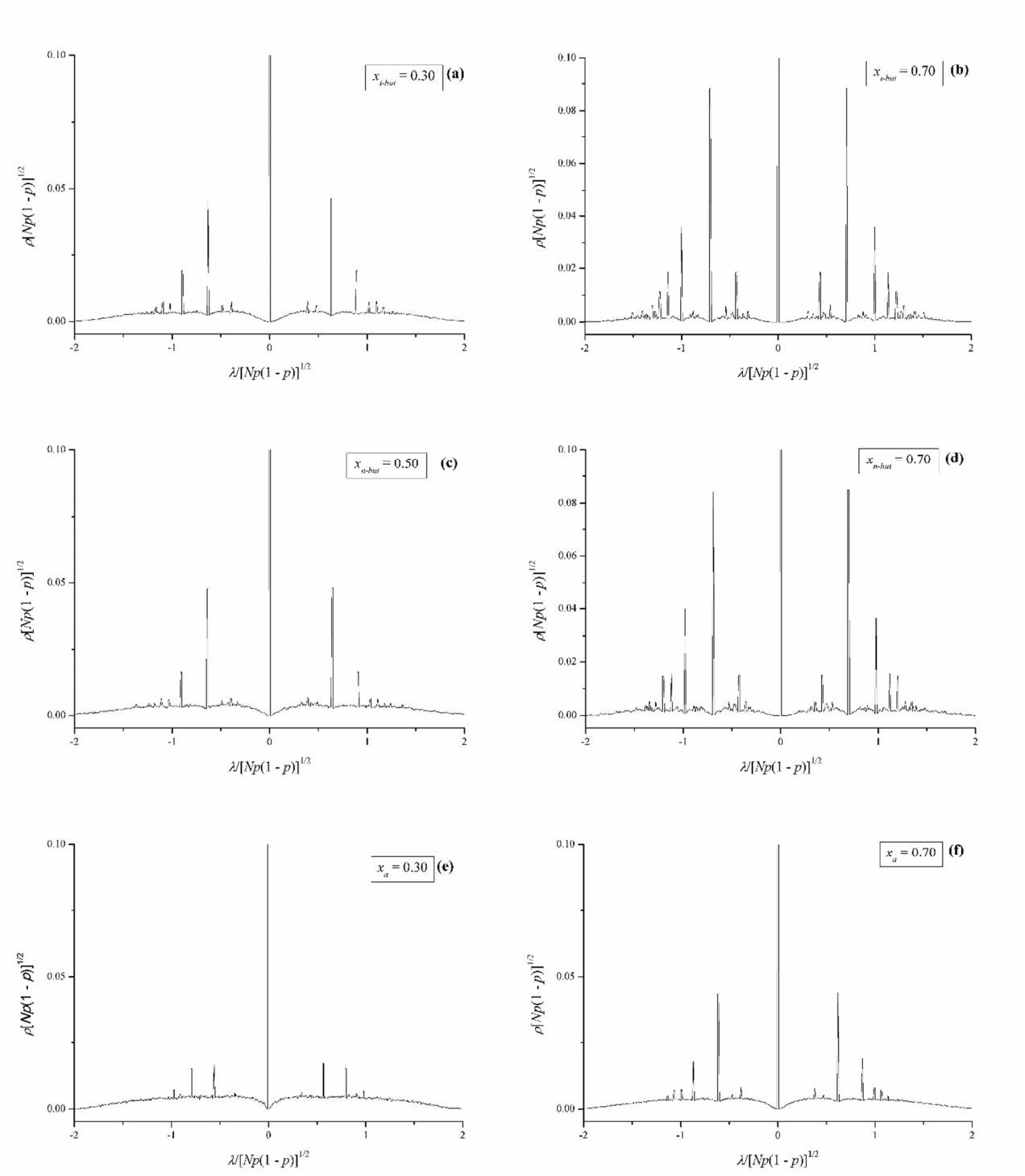

Fig. 9 Rescaled average spectral densities of H-bond networks in mixtures at selected compositions of *t*-butanol at 298.15 K (a) $x_{t\text{-but}} = 0.30$ and (b) $x_{t\text{-but}} = 0.70$; of *n*-butanol at 298.15 K (c) $x_{n\text{-but}} = 0.50$ and (d) $x_{n\text{-but}} = 0.70$; and of ammonia at 239.80 K (e) $x_a = 0.30$ and (f) $x_a = 0.70$. A cutoff value of 0.1 was used in the scaled spectral density in order to show more details.

Cite this: DOI: 10.1039/c0xx00000x

www.rsc.org/pccp

ARTICLE TYPE

Conclusions

The hydrogen bond (H-bond) networks generated from simulations of *t*-butanol, *n*-butanol and ammonia aqueous mixtures were analyzed by cluster (or island) statistics and topological statistical mechanics based properties. From island statistics we found that these H-bond networks change from a percolation regime for small solute concentrations (water rich mixtures) to a non-percolating behavior for non-aqueous component rich solutions. Topological analysis of local (clustering coefficients, average degrees) semi-global (path lengths) and global (spectral densities) properties indicated the presence of small-world patterns for the H-bond networks in the case of mixtures in the rich solute regime. In addition, the global features provided by the analysis of number of momenta in the spectral densities (number of peaks) correlates quite well with island statistics (rings, chains and branched chains) and other topological analyses performed in the water-alcohol and water-ammonia mixtures as well as with the observed small-world regimes. This corroborates the robustness of the statistical mechanics based topological analyses employed. The degree distributions of these networks were partially rationalized by the relative number and strengths of H-bonds formed by the solute molecules compared to those of water.

The presence of small-world topologies in a wide range of solute mole fraction of all mixtures studied suggests that small-world patterns may be common and general in complex H-bond networks of aqueous mixtures, probably due to their special features such as resilience and fast response to perturbations. This feature may be helpful in explaining and interpreting several physicochemical properties (thermochemistry, solubility, solute spectra, preferential solvation, etc.) of aqueous solutions.[1-8]

Acknowledgment

This work was partially supported by the Brazilian agencies CAPES, CNPq, FACEPE, FINEP, PRONEX-CNPq/FACEPE (APQ-0859-1.06/08), and inct-INAMI. Computational recourses from CENAPAD-PE are acknowledged. J. A. B. Silva thanks the CAPES/FACEPE for a post-doctoral fellowship.

Notes and references

[a] *Núcleo de Formação Docente, Centro Acadêmico do Agreste, Universidade Federal de Pernambuco, 55002-970, Caruaru, PE, Brazil.*
[b] *Departamento de Química Fundamental, Universidade Federal de Pernambuco, 50740-540, Recife, PE, Brazil. Fax: +55 81 21268442; Tel: +55 81 21268459; E-mail: longo@ufpe.br*
[c] *Departamento de Física Teórica e Experimental, Universidade Federal do Rio Grande do Norte, 59078-970, Natal, RN, Brazil*
[d] *Colegiado de Engenharia de Produção, Universidade Federal do Vale do São Francisco, 48902-300, Juazeiro, BA, Brazil*

1 A. Ben-Naim, *Solvation Thermodynamics*; Plenum: New York, 1987.
2 C. Reichardt, *Solvents and Solvent Effects in Organic Chemistry*; VCH: New York, 1990.
3 J. B. F. N. Engberts, *Water: Comprehensive Treatise*, 1979.
4 A. Wakisaka, T. W. Ebbesen, H. Sakuragi, K. Tokumaru, *J. Phys. Chem.*, 1987, **91**, 6547.
5 U. Kaatze, T. Telgmann, P. Miecznik, *Chem. Phys. Lett.*, 1999, **310**, 121.
6 A. K. Das, B. L. Tembe, *J. Mol. Liq.*, 1998, **77**, 131.
7 C. Liu, A. Bo.; G. Cheng, X. Lin, S. Dong, *Biochim. Biophys. Acta*, 1998, **1385**, 53.
8 I. -H. Um, Y. -M. Park, E. Buncel, *Chem. Commun.*, 2000, 1917.
9 V. M. L. Santos, F. G. B. Moreira, R. L. Longo, *Chem. Phys. Lett.*, 2004, **390**, 157.
10 J. A. B. Silva, F. G. B. Moreira, V. M. L. Santos, R. L. Longo, *Phys. Chem. Chem. Phys.*, 2011, **13**, 593.
11 J. A. B. Silva, F. G. B. Moreira, V. M. L. Santos, R. L. Longo, *Phys. Chem. Chem. Phys.*, 2011, **13**, 6452.
12 L. Dougan, S. P. Bates, R. Hargreaves, J. P. Fox, J. Crain, J. L. Finney, V. Réat, A. K. Soper, *J. Chem. Phys.*, 2004, **121**, 6456.
13 I. Bakó, T. Megyes, S. Bálint, T. Grósz, V. Chihaia, *Phys. Chem. Chem. Phys.*, 2008, **10**, 5004.
14 J. A. Morrone, M. E. Tuckerman, *J. Chem. Phys.*, 2002, **117**, 4403.
15 J. A. Morrone, K. E. Haslinger, M. E. Tuckerman, *J. Phys. Chem. B*, 2006, **110**, 3712.
16 S. Dixit, J. Crain, W. C. K. Poon, J. L. Finney, A. K. Soper, *Nature*, 2002, **416**, 829.
17 D. J. Watts, S. H. Strogatz, *Nature*, 1998, **393**, 440.
18 R. Albert, A.-L. Barabási, *Rev. Mod. Phys.*, 2002, **74**, 47.
19 M. W. Mahoney, W. L. Jorgensen, *J. Chem. Phys.*, 2000, **112**, 8910.
20 W. L. Jorgensen, *J. Phys. Chem.*, 1986, **90**, 1276.
21 W. L. Jorgensen, J. D. Madura, C. J. Swenson, *J. Am. Chem. Soc.*, 1984, **106**, 6638.
22 W. L. Jorgensen, *Encyclopedia of Computational Chemistry*, Wiley, New York, 1998, vol. 3, OPLS Force Fields, pp. 1986-1989.
23 R. C. Rizzo, W. L. Jorgensen, *J. Am. Chem. Soc.*, 1999, **121**, 4827.
24 L. C. G. Freitas, *J. Braz. Chem. Soc.*, 2009, **20**, 1541.
25 M. Pagliai, G. Cardini, R. Righini, V. Schettino, *J. Chem. Phys.*, 2003, **119**, 6655.
26 A. D. Boese, A. Chandra, J. M. L. Martin, D. Marx, *J. Chem. Phys.*, 2003, **119**, 5965.
27 R. F. i Cancho, C. Janssen, R. V. Solé, *Phys. Rev. E*, 2001, **64**, 046119-1.
28 D. Stauffer, A. Aharony, in *Introduction to Percolation Theory*, Taylor & Francis, London, 2nd ed., 1993.
29 L. A. N. Amaral, A. Scala, M. Barthélémy, H. E. Stanley, *Proc. Natl. Acad. Sci.*, 2000, **97**, 11149.
30 S. H. Strogatz, *Nature*, 2001, **410**, 268.
31 I. J. Farkas, I. Derényi, A. -L. Barabási T. Vicsek, *Phys. Rev. E*, 2001, **64**, 026704-1.
32 J. Gao, X. Xia, T. F. George, *J. Phys. Chem.*, 1993, **97**, 9241.
33 H. M. Cho, J. W. Chu, *J. Chem. Phys.*, 2009, **131**, 134107.
34 L. C. G. Freitas, *J. Mol. Struct. (Theochem)*, 1993, **282**, 151.
35 G. S. Kell, *J. Chem. Eng. Data*, 1975, **20**, 97.
36 R. C. Wilhoit, B. J. Zwolinski, *J. Phys. Chem. Ref. Data, Suppl.*,1973, 2.
37 E. S. Ferrari, R. C. Burton, R. J. Davey, A. Gavezzotti, *J. Comput. Chem.*, 2006, **27**, 1211.
38 J. Gao, D. Habibollazadeh, L. Shao. *J. Phys. Chem.*, 1995, **99**, 16460.
39 M. Ferrario, M. Haughney, I. R. McDonald, M. L. Klein, *J. Chem. Phys.*, 1990, **93**, 5156.
40 L. Haar, J. S. Gallagher, *J. Phys. Chem. Ref. Data*, 1978, 7, 635.
41 X. Wu, Y. Li, J. Lu, T. Teng, *Fluid Phase Equilibria*, 1992, **77**, 139.
42 W. L. Jorgensen, M. Ibrahim, *J. Am. Chem. Soc.*, 1980, **102**, 3309.
43 A. L. L. Sinoti, J. R. S. Politi, L. C. G. Freitas, *J. Mol. Struct. (Theochem)*, 1996, **366**, 249.
44 Y. Marcus, *Ion Solvation*, Wiley, New York, 1985.

45 V. S. Prasad, E. Rajagopal, N. M. Murthy, *J. Mol. Liq.*, 2006, **124**, 1.
46 J. Lara, J. E. Desnoyers, *J. Sol. Chem.*, 1981, **10**, 465.
47 A. K. Soper, F. Bruni, M. A. Ricci, *J. Chem. Phys.*, 1997, **106**, 247.
48 D. T. Bowron, J. L. Finnney, A. K. Soper, *J. Phys. Chem. B*, 1998, **102**, 3551.
49 A. H. Narten, *J. Chem. Phys.*, 1977, **66**, 3117.
50 J. W. Reed, P. M. Harris, *J. Chem. Phys.*, 1961, **35**, 1730.
51 M. Diraison, G. J. Martyna, *J. Chem. Phys.*, 1999, **111**, 1096.
52 M. A. Ricci, M. Nardone, F. P. Ricci, C. Andreani, A. K. Soper, *J. Chem. Phys.*, 1995, **102**, 7650.